

April 2019

Stretchable Battery Structures

Cesar A. Guerrero
Worcester Polytechnic Institute

Follow this and additional works at: <https://digitalcommons.wpi.edu/mqp-all>

Repository Citation

Guerrero, C. A. (2019). *Stretchable Battery Structures*. Retrieved from <https://digitalcommons.wpi.edu/mqp-all/7008>

This Unrestricted is brought to you for free and open access by the Major Qualifying Projects at Digital WPI. It has been accepted for inclusion in Major Qualifying Projects (All Years) by an authorized administrator of Digital WPI. For more information, please contact digitalwpi@wpi.edu.



Stretchable Battery Structures

A Major Qualifying Project
Submitted to the Faculty
of
WORCESTER POLYTECHNIC INSTITUTE
in partial fulfillment of the requirements for the
Degree in Bachelor of Science
in
Mechanical Engineering
By

Cesar Guerrero

Date: 4/25/2019
Approved by Project Advisor:

Provost Winston Soboyejo

This report represents work of WPI undergraduate students submitted to the faculty as evidence of a degree requirement. WPI routinely publishes these reports on its web site without editorial or peer review. For more information about the projects program at WPI, see <http://www.wpi.edu/project-based-learning>.

Abstract:

Stretchable energy-storage devices have attracted growing attention with the fast development of stretchable electronics, implantable medical devices, and paper display devices. However, the need for research in stretchable electronics that can sustain large mechanical strains while still maintaining their function is highly needed. Despite recent progress in stretchable electrodes, including, separator, sealing material, and conductive terminals remains a great challenge. That is why this project will focus on investigating different battery structures to create simple processes and designs for feasible scale-up manufacturing. This project also describes the fabrication and characterization of stretchable and conductive polymer nanocomposites embedded with carbon nanotubes (CNTs) and carbon black (CB) active materials for application of the anode in flexible lithium-ion batteries. To exhibit even higher levels of strain rate a buckling and divided method is performed. By understanding the mechanical properties of the buckling/wavy structure, we can incorporate high flexible properties while producing no significant reduction on their electronic properties and efficiency. It is demonstrated that the (CNT/CB)-embedded Poly(vinylidene fluoride) (PVDF) nanocomposites are capable of good electrical performance with mechanical flexibility, suggesting these nanocomposites could be outstanding anode candidates for use in flexible lithium-ion batteries.

Acknowledgements:

I would like to first thank Provost Winston Soboyejo for his guidance on this project. I would like to thank Oluwaseun Kehinde Oyewole PhD for mentoring and working alongside me, as well as helping me prepare samples and teaching me how to use the lab equipment to complete my experiments.

Table of Contents:

Abstract:	2
Acknowledgements:	3
Table of Contents:	4
Table of Figures	5
1. Introduction	6
2. Background	8
3. Methodology	9
Materials List:	9
PDMS Preparation Process:	9
PVDF preparation process	10
PEDOT:PSS preparation	10
PDMS using curing method	11
Buckling Process:	12
Casting method:	14
Buckled Stretchable Structures:	15
Divided packaging method	17
4. Results:	19
PVDF nanocomposite results:	19
Mechanical Test Results:	19
Tensile test results:	19
Fatigue Test results:	21
Electrical Resistance Testing	24
5. Conclusion:	25
6. Future Work	27
7. References	27

Table of Figures

Figure 1. Buckling Example	13
Figure 2 PDMS ribbed substrate	13
Figure 3 Prusa 3D Printer with ribbed substrate mold	14
Figure 4 Automatic film coater Casting PVDF nanocomposite	14
Figure 5 3D Printed Ribbed Dog Bone Structure Mold	15
Figure 6 dog-bone structure stretched	16
Figure 7 Buckled Stretchable Structure stretched	16
Figure 8 How the buckled structure was released from elongation	17
Figure 9 Divided Battery Structure	18
Figure 10 Divided Battery Structure Dog-Bone Sample	18
Figure 11 Divided Battery Structure Tensile Test Graph	20
Figure 12 Elongation at 35% Divided Battery Structure	20
Figure 13 Strain Equation	21
Figure 14 Graph 10% Strain Cycle	21
Figure 15 Graph 20% Strain Cycle	22
Figure 16 Graph 30% Strain Cycle	23
Figure 17 Graph 40% Strain Cycle	23
Figure 18 Graph of Resistivity under Fatigue	24

1. Introduction

Research on stretchable electronics is motivated by the need for electronic systems that can sustain large mechanical strain and still maintain their function. These stretchable devices can be wrapped conformally around complex and unconventional shapes, and have found applications in the biomedical fields, electronic paper display devices, sensor skins and photovoltaics. Within the biomedical fields, these electronics need to conform to body shape for use as wearables with a match in mechanical properties to minimize discomfort.¹ Extreme difficulties associated with the development of complete sets of stretch-able electronic materials force one to contemplate different types of mechanisms and structures to provide for a stretchable device. Stretchable electronics can be achieved in two ways: use of new structural layouts in conventional materials and new materials in conventional layouts.² The use of applying buckling mechanics to material layers could be beneficial for retaining their mechanical properties when stretched. Using this method while experimenting on innovative electrochemically stable materials could lead to interesting results in stretchable solar battery devices.

Current batteries are unable to sustain stable power, energy supply, and cyclic stability for uses under frequent mechanical strains, such as bending, twisting or other deformations. This is because the flexibility and strength of the electrodes is not high enough since inflexible materials are used; the contact among battery constituent materials is poor, operation at deformed states leads to severe degradation of the electrochemical and mechanical properties; and electrolyte leakage happens under certain circumstances.³ And thus, the development of mechanically strong flexible electrodes is most important factor to achieve a solution to the first problem.

This may be achieved by growing/embedding active electrode materials on fully flexible conductive substrates. This method involves blending active materials with a second electrochemically stable, electrically conductive, and mechanically strong composite. Three approaches were used for designing flexible electrodes. The first one is to cast (or deposit) active materials on a flexible substrate. The second is to paste an active material layer onto a stretched substrate using an epoxy adhesive, then release strained substrate to create buckles. And the last approach is to place two active material layers perpendicular to the substrate leaving a gap of about 5 mm in between. Then adding a layer of uncured substrate to fully seal the material.

Using these methods of flexible conductive substrates, it is possible to avoid using electrode and metal foils since it is how batteries are being manufactured today. Using substrates instead of foils would reduce the overall energy densities of a full LIB as the substrate would account for over 15% of the total mass of the electrode with no contribution to lithium storage.⁴ Second, the metal foils have low surface areas, thus exhibit weak adhesion and limited contact to the active material. As such, gaps may be formed at the electrode– metal interface resulting from volumetric change of the active materials during the charge and discharge processes at higher rates. Thus, battery performances may undergo degradation both in capacity and cyclic stability. Using conductive flexible substrates having excellent flexibility and mechanically strong would solve these problems in adhesions and degradation as well as lowering the total mass of the electrodes for an ideal flexible battery. ⁵

2. Background

Recently, there has been an emerging interest in stretchable power sources including energy storage and energy harvesting. Energy storage devices, including batteries and supercapacitors, play an important role in powering systems of portable electronic devices or implantable medical devices. There are also a plethora of uses for these energy harvesting devices such as the development of soft portable electronic devices, such as rollup displays, wearable devices, radio-frequency identification tags, and integrated circuit smart cards.

Flexible batteries have a history of almost 100 years. Earlier studies focused on flexible alkaline batteries³⁻⁶ and all-polymer batteries (or plastic batteries).⁷⁻¹¹ Later, polymer lithium-metal batteries began to gain more interest.¹²⁻¹⁵ Recent research interest is being intensively concentrated on flexible LIBs.¹⁶⁻¹⁸ Compared to other types of batteries, flexible LIBs possess higher energy density, higher output voltage, longer life and environmentally benign operation, etc.¹⁹ Flexible LIBs share the same principles of “conventional” LIBs, which have been described in many papers.¹⁸⁻¹⁹ So far, not only has great progress been made in the development of the core battery composites: electrode materials, shape-conformable solid electrolytes, and soft and mechanically strong current collectors, significant advances have also been achieved in the battery design. Many novel technologies and processes have been invented to make flexible electrodes and to fabricate full batteries with high performance. The materials development has been considerably spurred by the advances in nanoscience and nanotechnology, which offer many different kinds of novel one-dimensional (1D) and two-dimensional (2D) nanosized materials such as nanostructured carbon (nanotubes, carbon fibers, and graphene), nanostructured silicon (nanoparticles (NPs) and nanowires (NWs)), nanostructured metal oxides, and nanostructured conventional cathode materials, etc. The invention/introduction of conventional or new technologies and processes such as self-assembly, sputtering, deposition, painting, and printing, in turn, brings advances in the electrode materials research and development.²⁰⁻²⁴ Nevertheless, the challenges for flexible LIBs research are still huge.

Current batteries are unable to sustain stable power and energy supply and cyclic stability for uses under frequent mechanical strains, such as bending, twisting or other deformations. This mostly results from: The flexibility and strength of the electrodes not high enough because intrinsically inflexible materials are used; The contact among battery constituent materials is poor, particularly the active materials–substrate contact; operation at deformed states leads to severe degradation of the electrochemical and mechanical properties; and electrolyte leakage happens under certain circumstances, and thus, the development of mechanically strong flexible electrodes is required. This may be achieved by embedding/mixing active electrode materials on fully flexible conductive substrates without the use of conductive additives or binders. Flexible polymer solid electrolytes with optimal mechanical properties and ionic conductivity still need to be developed. Optimization of battery production and packaging in order to increase productivity and reduce cost, for which advanced process technologies should be introduced and adopted.

The use of carbon nanotubes for active materials in the nanocomposite is very advantageous. It could be used for the battery's anode and current collectors for its excellent conductivity and lithium intercalation. Carbon nanotubes are used for strengthening properties as well giving the polymer composite and enhanced tensile strength. The different process of creating these structures are discussed in the methodology.

3. Methodology

Materials List:

Poly(vinylidene fluoride) average Mw ~534,000 by GPC, powder ; Triton X-100 4-(1,1,3,3-Tetramethylbutyl)phenyl-polyethylene glycol; Dimethyl Sulfoxide (DMSO) ; PEDOT:PSS, Poly(2,3-dihydrothieno-1,4-dioxin)-poly(styrenesulfonate) ; Carbon Nanotube, multi-walled carbon >95% L 6-9 nm x 5 um. All acquired from sigma aldrich. 184 silicone elastomer and curing agent to produce Poly(dimethylsiloxane) PDMS bought from sylgard brand. Conductive carbon black EQ-lib-superC65. 3D solutech PLA filament.

PDMS Preparation Process:

The device structure is comprised of a substrate and an active electrode layer nanocomposite on top of the substrate. The materials for the substrate will be Poly(dimethylsiloxane) or PDMS. This polymer material has a silicone base, is highly-stretchable, and is a non-toxic polymer, perfect for use as a substrate for the electrode nanocomposite. It is made from a silicone base and curing agent using a 10:1 ratio.

PDMS substrate process

- Syringe to extract 6 mg of Silicone base
- Syringe with needle to extract 0.6 mg of curing agent
- Mix base and curing agent in container for 2 mins
- Pour mixture in impermeable mold of desired thickness and shape
- Degassing uncured PDMS to remove all bubbles (~15 mins)
- Cure degassed PDMS at 60 °C for 2 hours in oven

PVDF preparation process

The process to create a polymer nanocomposite for the lithium ion battery was determined. Several iterations, as explained below in greater detail, were performed to determine and discover appropriate experiment parameters to create the composite anode. First the Polyvinylidene fluoride (PVDF) polymer material was developed, then the mixture of carbon nanotubes and Carbon black was added.

PVDF Preparation

Ratios:

8:1:1 Ratio of PVDF : Carbon Nanotubes : Carbon Black

20 mg of PVDF / 1 mL - NMP

PVDF polymer Preparation:

- Pipet 4 mL of NMP
- Stir NMP with Magnetic magnet
- Add 80 mg of PVDF pellets
- Wrap bottle in aluminum foil (NMP sensitivity to light)

Composite Preparation:

- Dry Sonicate 10mg of CNT & 10 mg CB for 1 hour
- Add sonicated CNT/CB into PVDF solution
- stir @ 900 rpm for 1 hour

PEDOT:PSS preparation

PEDOT:PSS was bought in liquid form and ready to be cast or spin coated. But before deposited on the PDMS substrate, the PEDOT:PSS had to be treated to be more hydrophilic using standard chemical treatment procedure. PEDOT:PSS was treated using DMSO and Triton-X and using spin coated on the PDMS substrate at 1500 rpm for 30 seconds.

Ratios:

8:1:1

PEDOT:PSS: 80 mg

Carbon Nanotubes (CNT): 10 mg

Carbon Black (CB): 10 mg

Composite Preparation:

- Dry Sonicate 10mg of CNT & 10 mg CB for 1 hour
- Add sonicated CNT/CB into PEDOT:PSS solution
- Pipet 150 uL of DMSO solution into PEDOT:PSS mixture
- Pipet 430 of Triton X-100 solution into PEDOT:PSS mixture
- Stir for 1 hr @ 900 rpm

PDMS using curing method

The PDMS curing method is a processing method developed to eliminate the adhesion of two different polymers by using the same polymer as the substrate and matrix of the electrode. This process consists of making a PDMS, substrate leaving it semi cured, and adding another layer of the PDMS nanocomposite on the surface of the uncured substrate, curing both simultaneously, but leaving the anode nanocomposite layer on top without it being intermixing with the PDMS substrate.

PDMS Curing Method Process:

Ratios:

8:1:1 ratio of PDMS -(CNT/CB) mixture

PDMS: 75 mg

Carbon Nanotubes (CNT): 12.5 mg

Carbon Black (CB): 12.5 mg

PDMS substrate process:

- Syringe to extract 6 mg of Silicone base
- Syringe with needle to extract 0.6 mg of curing agent
- Mix base and curing agent in container for 2 mins
- Pour mixture in impermeable mold of desired thickness and shape

- Degassing uncured PDMS to remove all bubbles (~15 mins)
- Cure degassed PDMS at 60 °C for 1 hour in oven (leaving PDMS semi-cured)

Composite Preparation:

- Dry Sonicate 10mg of CNT & 10 mg CB for 1 hour
- Add sonicated CNT/CB into PDMS solution
- Stir for 1 hr @ 900 rpm

Final Process:

- Spin coat PDMS nanocomposite into semi-cured PDMS substrate
 - Spin coat 1500 rpm for 30 seconds
- Put PDMS substrate & electrode nanocomposite into oven at 60° C
- Cure structure for 2 hours

Unfortunately, the PDMS nanocomposite was not conductive, making for an unsuitable electrode nanocomposite. No further analysis or testing was done on this sample. This process could be beneficial for use in different flexible electronic applications where using one polymer for the substrate and composite is needed.

Buckling Process:

The buckling method in figure 1 is a simple stretch and release process where the stretchable substrate is stretched at a given strain, a layer is adhered to the substrate and then the substrate is released causing buckles or wrinkles to the layer on top. This is used to give the desired stretchable properties and strain to materials that cannot reversibly extend to the desired amount.

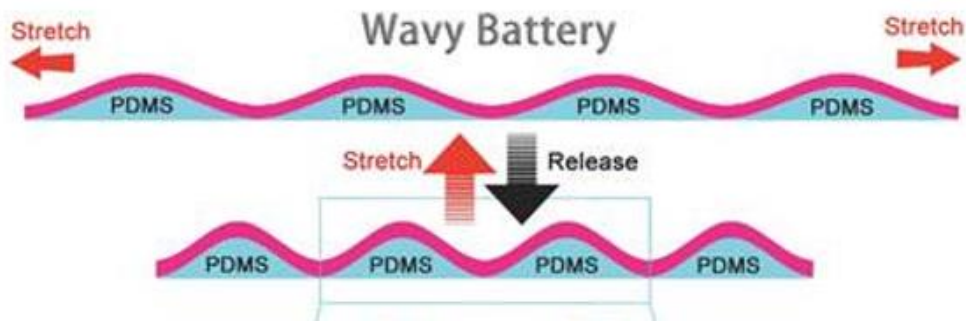


Figure 1. Buckling Example

An alternate buckling method was used to satisfy adhesion problems with the PVDF anode nanocomposite. In this method there is 2mm ribs in the substrate being 2mm in length and having 1.6mm of spacing in-between them. (Fig .2) An epoxy adhesive was placed on the surface of each rib to attach the PVDF anode nanocomposite onto the substrate. The stretch and release process are the same, but because of the gaps in between the ribs, the buckle's length is exactly the same as the gaps of the substrate, which is 6 buckles of 1.6mm each.

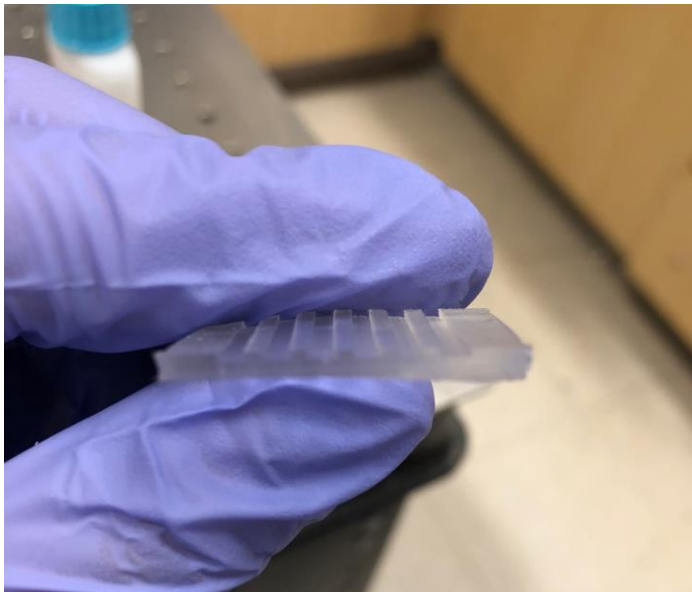


Figure 2 PDMS ribbed substrate

The molds for the substrates had to be custom 3D printed to satisfy the specification of the substrate. Using SolidWorks as a Computer Aided design software, the mold was designed being able to contain 3 samples. A Prusa 3D printer was used to print this mold in PLA plastic. (fig. 4)

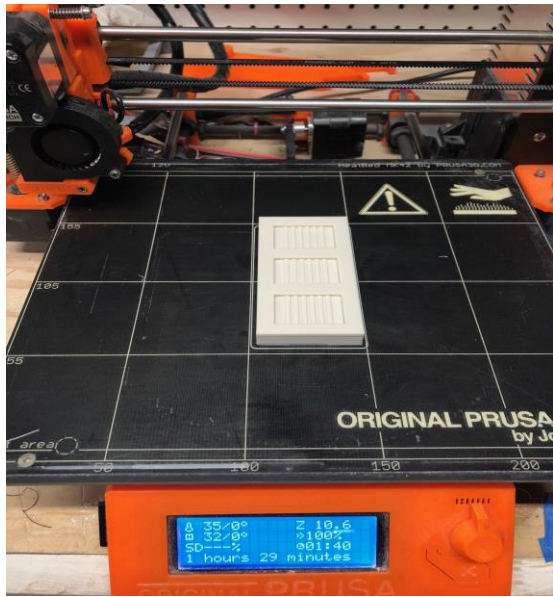


Figure 3 Prusa 3D Printer with ribbed substrate mold

Casting method:



Figure 4 Automatic film coater Casting PVDF nanocomposite

The PVDF anode nanocomposite was fabricated using a casting method (Fig 4). The liquid mixture was cast using an automatic film coater set at a thickness of 150 μm on aluminum foil or hydrophobic polymer sheet having for the ability to be peeled off. After casting the PVDF nanocomposite would fully dry in 25 mins at room temperature or 15 mins at 60 $^{\circ}\text{C}$.

Buckled Stretchable Structures:

To test buckled samples, the polymer substrate had to be modified. Making a second iteration of the substrate mold, a dog bone design was implemented (Fig 5). Having the same ribbed dimensions and spacing the main design change was the two large ends to have better grip when doing mechanical testing on the samples.

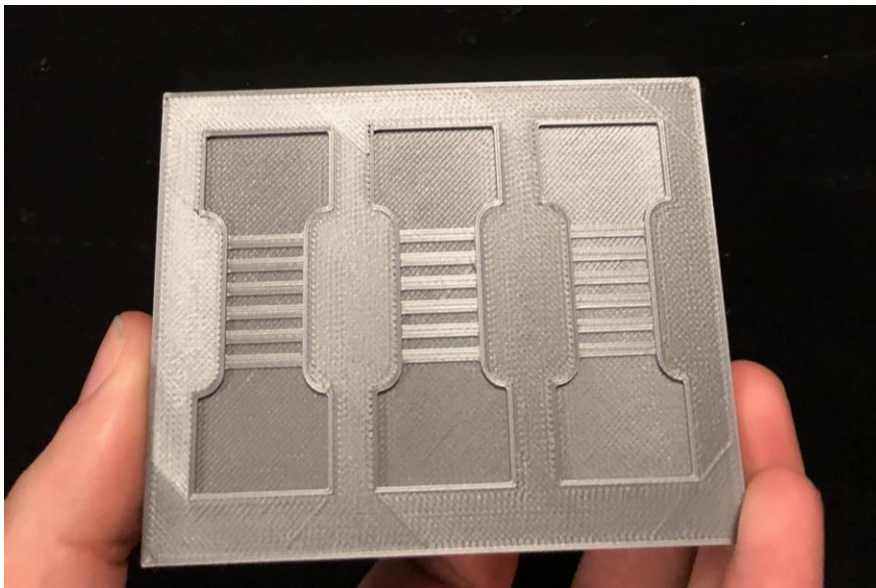


Figure 5 3D Printed Ribbed Dog Bone Structure Mold

The dog bone structures were stretched to 40% strain and kept in position by two clips. (Fig 6). A layer of epoxy adhesive was added to each of the 6 ribs. Then the anode nanocomposite is deposited on the ribs of the substrate and pressed specifically on those 6 ribs. (Fig 7). After 1 hour of letting the epoxy cure, the substrate was released from the clip and buckling occurred on the anode nanocomposite. (Fig. 8).

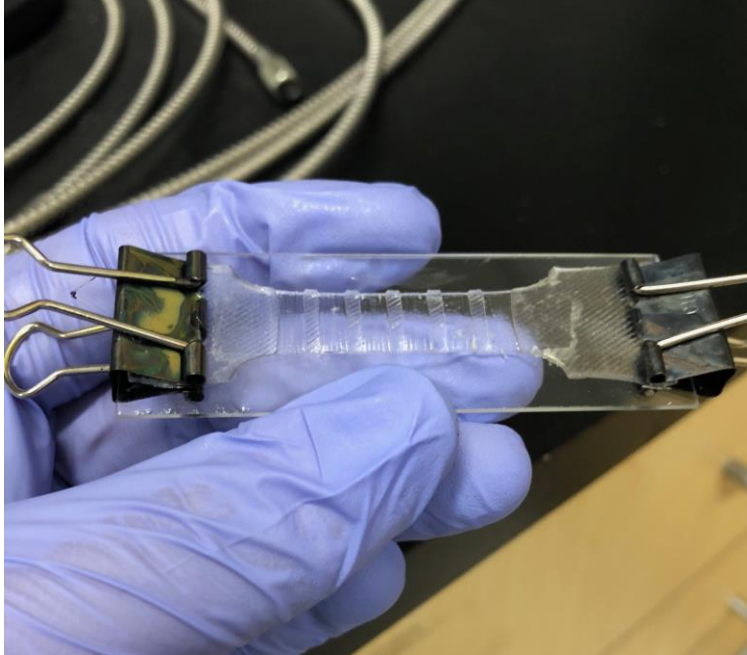


Figure 6 dog-bone structure stretched

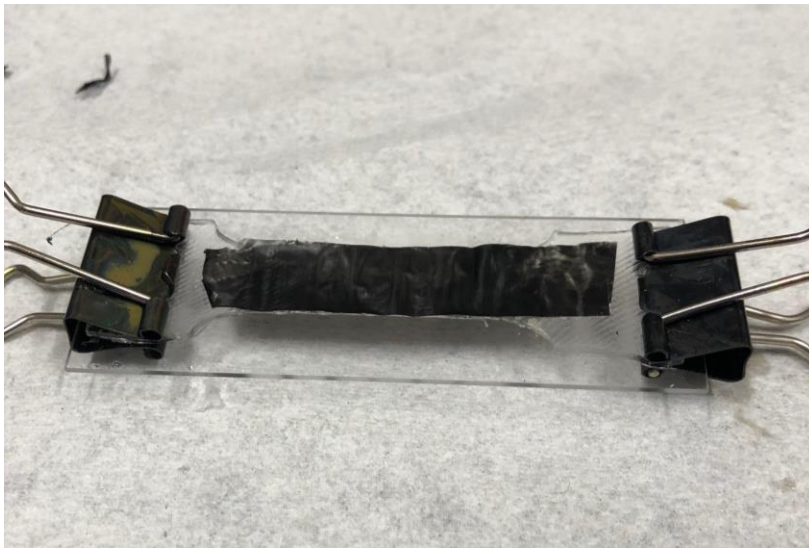


Figure 7 Buckled Stretchable Structure stretched

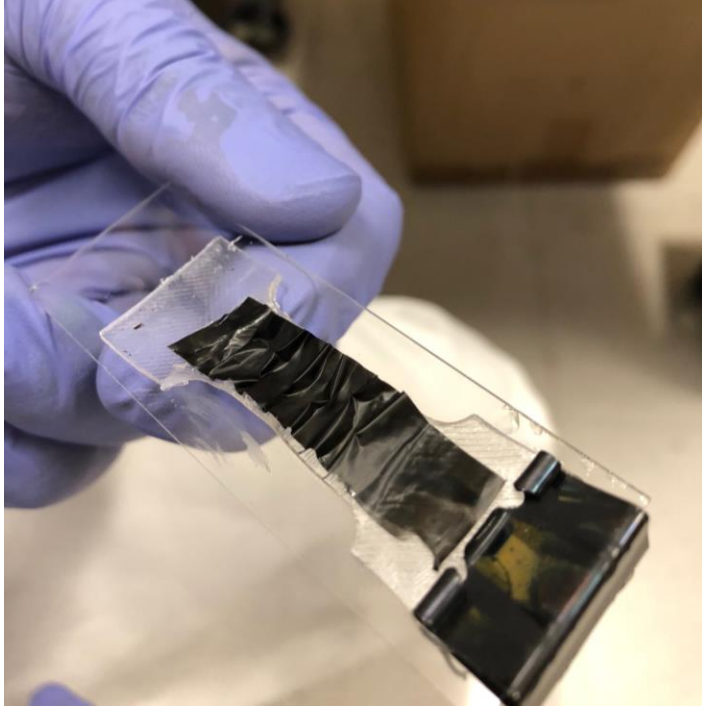


Figure 8 How the buckled structure was released from elongation

Divided packaging method

The divided battery structure was another process designed to fully adhere and minimize the stress on the electrode layer. Strips of anode nanocomposite were placed perpendicular to the PDMS substrate leaving a ~5mm gap in-between the two nanocomposite strips. Then a thin layer ~1mm thick of uncured PDMS was applied to the top of entire structure. The PDMS will cure and produce a secure, stretchable structure leaving no form of delamination of the substrate.

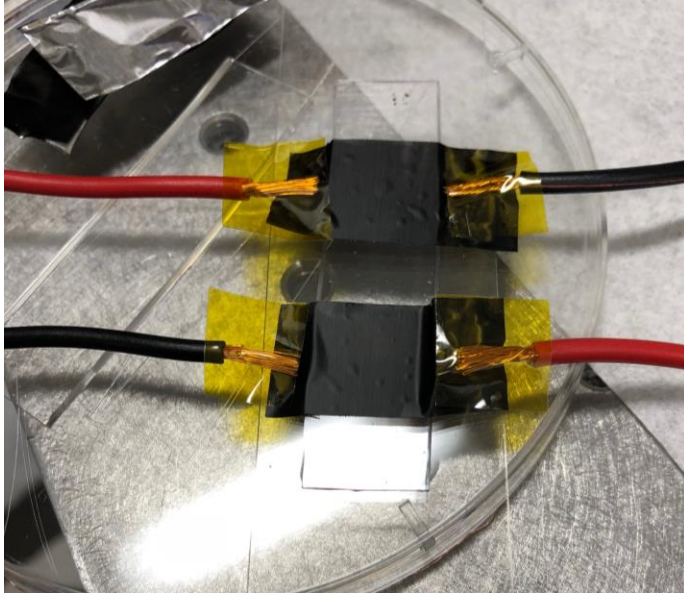


Figure 9 Divided Battery Structure

The device was measured through the resistance in the anode nanocomposite terminals that are connected to wires. The device underwent fatigue tests while values of resistance were measured through a multimeter and recorded through every cycle. (Fig 9)

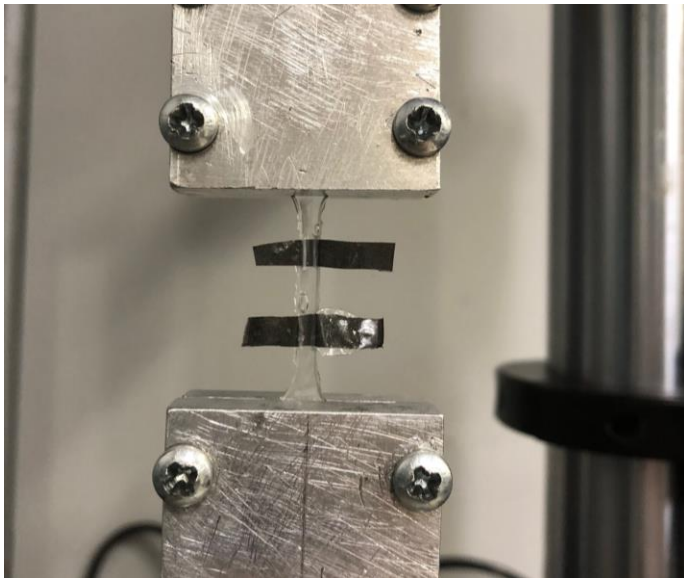


Figure 10 Divided Battery Structure Dog-Bone Sample

Several samples were tested adopting a thinner dog-bone structure and placed in an Instron micro-tensile machine for more accurate fatigue measurements on small samples. This machine

used to do tensile and fatigue tests on these dog bone samples seen in figure 10 before the wires were attached to the terminal ends.

4. Results:

PVDF nanocomposite results:

PVDF is the optimal polymer matrix for CNT & Carbon Black electrode. The PDMS-CNT/CB nanocomposite was not conductive at all, and the PEDOT:PSS-CNT/CB nanocomposite could not retain the carbon nanotubes or carbon black very well in its matrix. The PVDF-CNT/CB nanocomposite was able to exhibit conductivity as well as excellent retention of the active material in its matrix, since it is used as the standard binder for lithium-ion battery electrodes. For this reason, PVDF was the only matrix of the anode nanocomposite used in the mechanical testing of the buckling and divided stretchable structures.

Mechanical Test Results:

Testing of the mechanical properties were performed on the device when it is fatigued, strained and deformed. Tests were conducted on both buckled and divided stretchable structures. However, after the first set of fatigue cycles tests, the buckled battery structures would produce significant delamination. Therefore, no qualitative data were able to be presented on the buckled nanocomposite structures. Several samples of the divided stretchable structures were tested, doing tensile tests until failure, and fatigue tests of a total of 800 cycles per sample.

Tensile test results:

Tensile tests were done on a PDMS 20mm long, 3mm wide, and 3mm thick substrate. The two anode nanocomposite layers embedded 1 mm thick in the substrate. The anode nanocomposite layers were both 3mm in length with a 5mm gap in-between the two layers. The tensile test was conducted at 1mm/sec time of elongation.

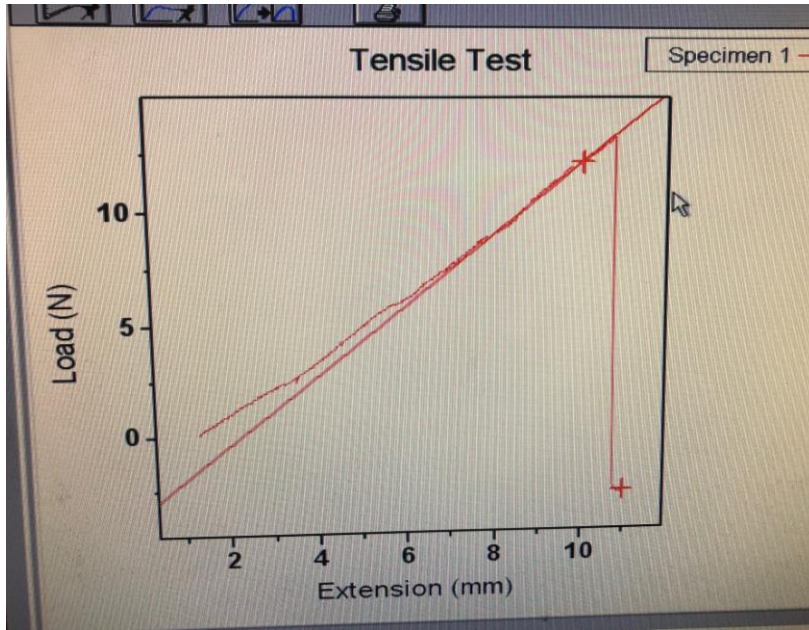


Figure 11 Divided Battery Structure Tensile Test Graph

As seen in figure 11 the tensile graph was very interesting. The PDMS substrate exhibits reversible strain without any plastic deformation until the samples point of failure where it snapped at 10.8mm or approx 54% strain. During the sample being strained the anode nanocomposite layers were completely stable showing no form of flexure during the whole process.

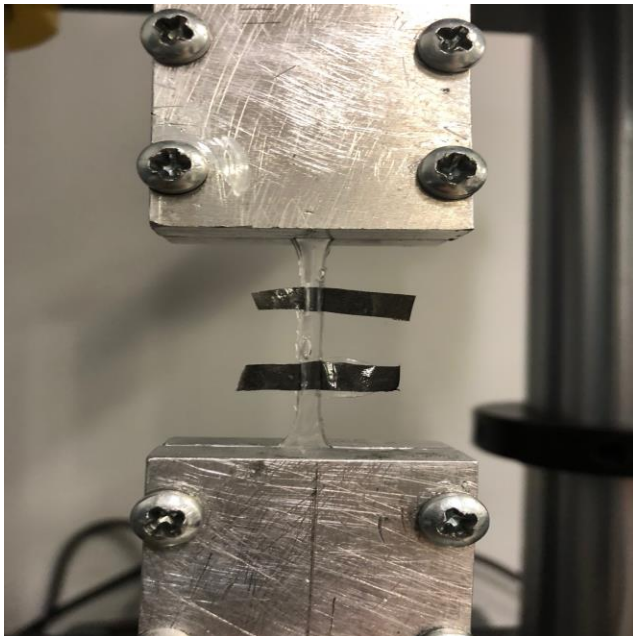


Figure 12 Elongation at 35% Divided Battery Structure

The anode nanocomposite in figure 12 showed very little deformation or flexure at 7mm of deformation or 35% strain. This is because of the process used to seal the anode nanocomposite. Curing a 1mm layer of PDMS on top of the anode nanocomposite does not let it deform while inside the PDMS layer since it does not let it exceed dangerous levels of strain where the anode nanocomposites would deform.

$$strain = \frac{\Delta L}{L}$$

Figure 13 Strain Equation

The tensile and fatigue sample's strain rates were determined through the simple strain equation shown in Figure 13.

Fatigue Test results:

The various samples of the divided stretchable structure were tested using standard fatigue tests in the instron micro-tensile machine. Each sample went under a total of 800 fatigue cycles. The samples started at 10% and every 200 cycles, the strain rate increased by 10% linearly, testing the sample at 10%, 20%, 30%, 40% strain rates respectively.

Graph of 10% strain cycle

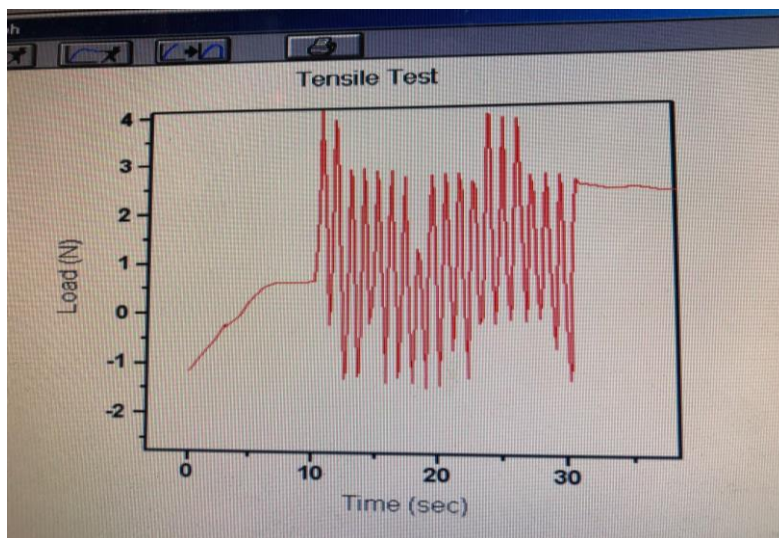


Figure 14 Graph 10% Strain Cycle

- Sample of 25 load cycles @ 10% strain (Fig 14)
- 2mm strain rate on 20mm sample raised 1.5mm, then cycled 0.5 mm up and -0.5 down.

Graph of 20% strain cycle

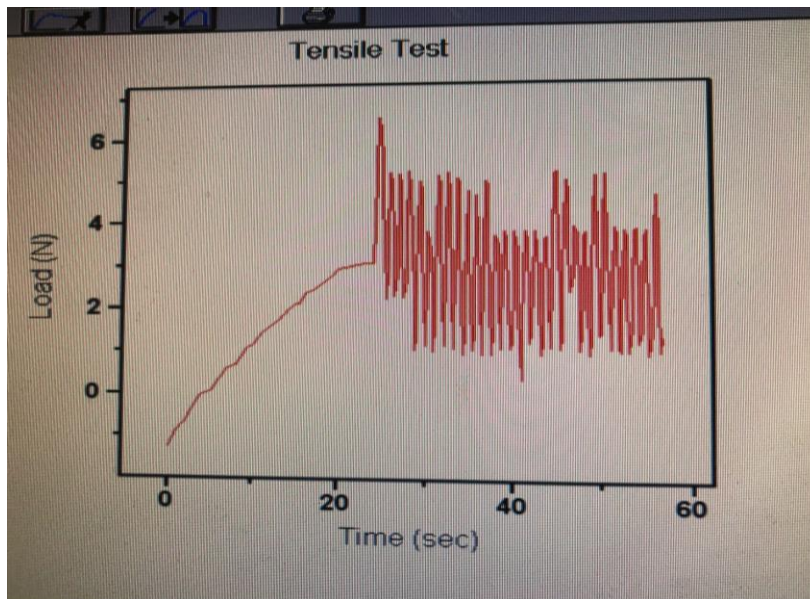


Figure 15 Graph 20% Strain Cycle

- Sample of 25 load cycles @ 20% strain (Fig. 15)
- 4mm strain rate on 20mm sample raised 3mm, then cycled 1mm up and -1mm down.

Graph of strain 30%

Graph of 30% strain cycle

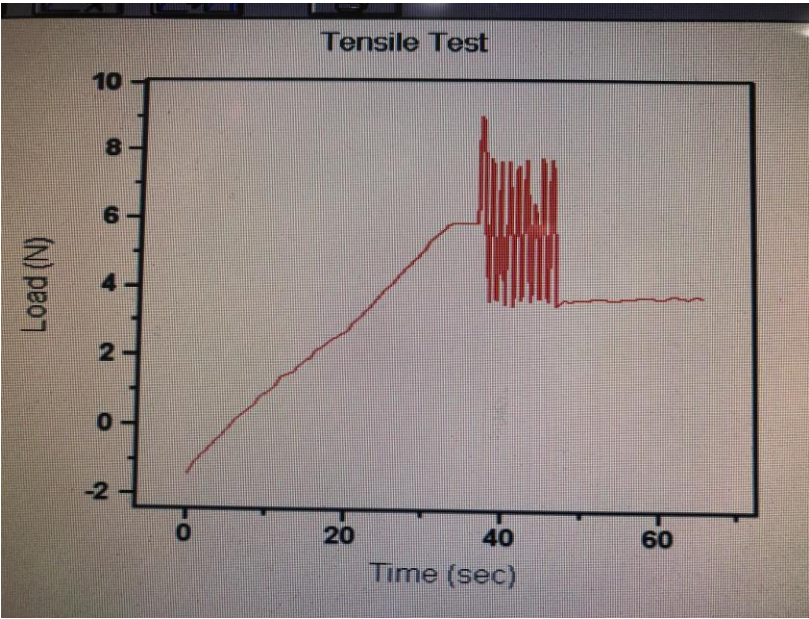


Figure 16 Graph 30% Strain Cycle

- 6 mm strain rate on 20mm sample raised 5mm, then cycled 1mm up and -1mm down

Graph of 40% strain cycle

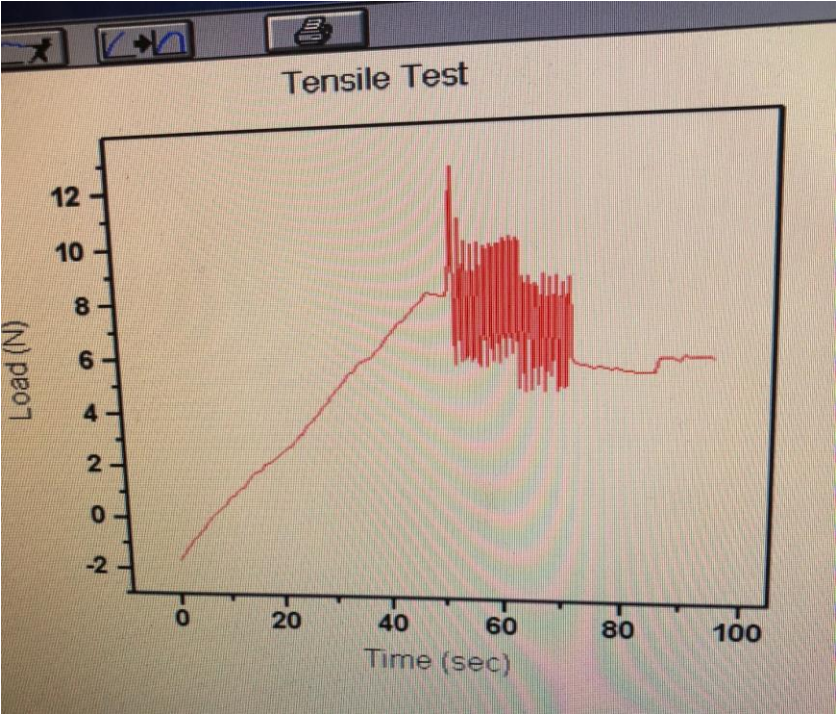


Figure 17 Graph 40% Strain Cycle

- 8mm strain rate on 20mm sample raised 7mm, then cycled 1mm up and -1mm down.

Electrical Resistance Testing

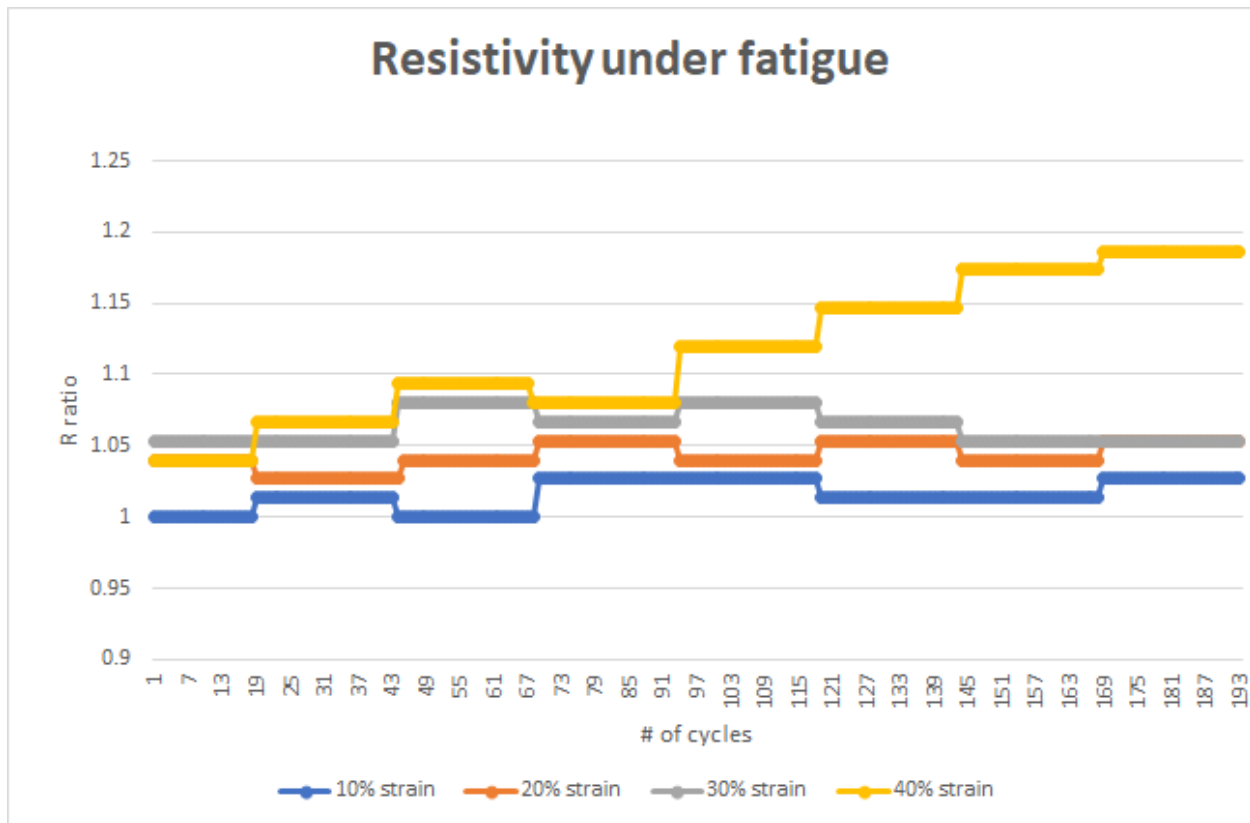


Figure 18 Graph of Resistivity under Fatigue

The resistance of the divided stretchable samples was measured and studied while being fatigued. Only the resistance was measured to produce a qualitative study not just on battery structures, but also applicable to different structures such as LEDs, solar cells, or sensors.

This graph (Fig. 18) explains the resistance measurements at 10%, 20%, 30%, and 40% strain cycling of the full divided stretchable structure. The ratio of R is R_j / R_0 where R_j is the resistance of the devices after N cycles, and R_0 is the standard resistance measured before fatigue of device. The resistance R_j was measured after every 25 cycles of the fatigued sample until the final measured 200 cycles. This was done for each of the four strain rates tested.

It was found that the resistance did not vary significantly for the 10%, 20% and 30% strains. At 10% strain cycling the system increased very little in resistance (2k Ω) out of 75 k Ω of resistance, meaning there was only a 2.6% increase in resistance. At 20% strain cycling the system only increased 3 Ω very close to the 10% strain cycling. These strain rates it did not exceed 1.05x the resistance of the system which is the safety factor placed on this anode structure, meaning it would have negligible effects on performance on the battery system. At 30% strain cycling, the maximum increase in resistance was 6k Ω . Although it is only an 8% increase, and it does not exceed 1.1x resistance ratio, it would not be suitable for a battery system since it would affect the battery performance, or charging and discharging rates. When measuring the resistance at 40% strain rate cycles, the resistance of the system was linearly larger. The other strain rates had somewhat random variation of the resistances over the increasing number of cycles, but 40% strain cycling had increasing variation after approximately 100 cycles. The increase in resistance was 14% in total which would alter the charging and discharging time, impacting battery performance, but not by a significant amount.

5. Conclusion:

In conclusion all three processing methods produced a high reversible strain of ~30-40% of 40mm structure. The PDMS curing method was not tested because the PDMS anode nanocomposite was not conductive, although it would have similar properties to the PDMS substrates tested and would produce high strain rates. The alternate stretchable buckling method using an epoxy adhesive and a ribbed PDMS substrate would produce reversible strain rates of 40% strain without tearing or fracturing the anode nanocomposite, but it had several delamination problems when fatigue cycle tested ~25-50 cycles. The divided stretchable structure was able to be fatigue cycle tested for 800 cycles producing no tearing or fracture in either the anode nanocomposite or substrate.

PVDF proved to be the optimal polymer matrix for CNT & Carbon Black electrode. The PEDOT:PSS-CNT/CB nanocomposite could not retain the carbon nanotubes or carbon black very well in its matrix, and The PDMS-CNT/CB nanocomposite was not conductive at all. The PVDF-CNT/CB nanocomposite was able to exhibit conductivity as well as excellent retention of the active material in its matrix, since it is used as the standard binder for lithium-ion battery electrodes.

The divided stretchable structure produced significantly less stress and current variation to the electrode material than the buckling stretchable structure, mainly because the entire buckling structure is deforming back and forth while testing, when the divided stretchable structure was only partially deforming since most of the deformation was done on the PDMS substrate instead of the anode material, due to the design of the structure. Problem of delamination were fixed using the divided stretchable structure method. Since this method is uses the same PDMS polymer to seal the anode nanocomposite.

With the divided stretchable structure at 10-20% strain the anode material does not exhibit a very big difference in resistance. More so, the images show that the anode material does not seem deformed and no delamination occurs. Through these assumptions, the material at 10-20% strain would not affect the performance of the anode material in a lithium ion battery. A conventional anode with only 5% polymer binder matrix could be feasible using the divided stretchable structure processes if it would not exceed 10-20% strain. While 30-40% strain cycle did not have a significant change in resistance, it would still affect the battery systems performance when charging and discharging.

Since the ratio of polymer matrix to active material (8:1:1) had good mechanical properties but low conductivity. It is recommended using smaller ratio of polymer mix so that the composite could work as an electrode and current collector since the resistivity measured in the nanocomposite is still very high compared to the resistivity of battery current collectors.

These processing methods could prove to be advantageous when trying to manufacture different electronic wearable devices. The best processing method to use for wearable electronics would be the divided stretchable structure because of its low stress on the device and high reversible strain rates causing negligible resistance at 10-20% strain cycling. This method produced successful processing methods for scale-up stretchable battery structures and other wearable devices.

6. Future Work

- Different treating methods for PVDF composite to adhere better to PDMS.
- Investigate better adhesion materials between PVDF and PDMS.
- Conduct more experiments with curing process.
- Fabricate a full battery on buckled and divided stretchable structures
- Use some/all of these processing methods for stretchable devices.
- Produce dynamic electrochemical tests on stretchable battery full-cell/half cell.

7. References

1. H. Nishide and K. Oyaizu , *Science*, 2008, **319** , 737 -738 [CrossRef](#) [CAS](#) [PubMed](#)



2. A. Nathan , A. Ahnood , M. T. Cole , S. Lee , Y. Suzuki , P. Hiralal , F. Bonaccorso , T. Hasan , L. Garcia-Gancedo , A. Dyadyusha , S. Haque , P. Andrew , S. Hofmann , J. Moultrie , D. Chu , A. Flewitt , A. Ferrari , M. Kelly , J. Robertson , G. Amaratunga and W. Milne , *Proc. IEEE*, 2012, **100** , 1486 -1517 [CrossRef](#)



3. A. M. Biggar 1968



4. A. M. Gaikwad , A. M. Zamarayeva , J. Rousseau , H. Chu , I. Derin and D. A. Steingart , *Adv. Mater.*, 2012, **24** , 5071 -5076 [CrossRef](#) [CAS](#) [PubMed](#)



5. A. M. Gaikwad , G. L. Whiting , D. A. Steingart and A. C. Arias , *Adv. Mater.*, 2011,

23 , 3251 -3255 [CrossRef](#) [CAS](#) [PubMed](#)



6. Z. Q. Wang , Z. Q. Wu , N. Bramnik and S. Mitra , *Adv. Mater.*, 2014, **26** , 970 -

976 [CrossRef](#) [CAS](#) [PubMed](#)



7. T. Nagatomo , C. Ichikawa and O. Omoto , *J. Electrochem. Sci.*, 1987, **134** , 305 -

308 [CrossRef](#) [CAS](#) [PubMed](#)



8. Y. Gofer , H. Sarker , J. G. Killian , T. O. Poehler and P. C. Searson , *Appl. Phys.*

Lett., 1997, **71** , 1582 -1584 [CrossRef](#) [CAS](#) [PubMed](#)



9. I. Sultanaa , M. Rahman , J. Wang , C. Wang , G. G. Wallace and H. K. Liu ,

Electrochim. Acta, 2012, **83** , 209 -215 [CrossRef](#) [PubMed](#)



10. J. C. Killian , B. M. Coffey , F. Gao , T. O. Poehler and P. C. Searson , *J.*

Electrochem. Soc., 1996, **143** , 936 -942 [CrossRef](#) [CAS](#) [PubMed](#)



11. L. Nyholm , G. Nyström , A. Mihranyan and M. Strømme , *Adv. Mater.*, 2011, **23** ,

3751 -3769 [CrossRef](#) [CAS](#)



12. J. H. Shin , M. A. Henderson and S. Passerini , *J. Electrochem. Soc.*, 2005, **152** ,

A978 -A983 [CrossRef](#) [CAS](#) [PubMed](#)



13. M. Mastragostino , F. Soavi and A. Zanelli , *J. Power Sources*, 1999, **81** , 729 -











733 [CrossRef](#)



14. L. Sannier , R. Bouchet , S. Grugeon , E. Naudin , E. Vidal and J. M. Tarascon , *J.*

Power Sources, 2005, **144** , 231 -237 [CrossRef](#) [CAS](#) [PubMed](#)



15. A. Abouimrane , Y. Abu-Lebdeb , P. J. Alarco and A. Armand , *J. Electrochem. Soc.*, 2004, **151** , A1028 -A1031 [CrossRef](#) [CAS](#) [PubMed](#)  .
16. H. Gwon , J. Hong , H. Kim , D. H. Seo , S. Jeon and K. Kang , *Energy Environ. Sci.*, 2014, **7** , 538 -551 [CrossRef](#) [CAS](#)  .
17. S. Y. Lee , K. H. Choi , W. S. Choi , Y. H. Kwon , H. R. Jung , H. C. Shin and J. Y. Kim , *Energy Environ. Sci.*, 2013, **6** , 2414 -2423 [CrossRef](#) [CAS](#)  .
18. G. Zhou , F. Li and H. H. Cheng , *Energy Environ. Sci.*, 2014, **7** , 1307 -1338 [CrossRef](#) [CAS](#)  .
19. M. Armand and J. M. Tarascon , *Nature*, 2008, **451** , 652 -657 [CrossRef](#) [CAS](#) [PubMed](#)  .
20. S. W. Lee , B. M. Gallant , H. R. Byon , P. T. Hammond and Y. Shao-Horn , *Energy Environ. Sci.*, 2011, **4** , 1972 -1985 [CrossRef](#) [CAS](#)  .
21. S. W. Lee , B. M. Gallant , Y. M. Lee , N. Yoshida , D. Y. Kim , Y. Yamada , S. Noda , A. Yamada and Y. Shao-Horn , *Energy Environ. Sci.*, 2012, **5** , 5437 -5444 [CrossRef](#) [CAS](#)  .
22. V. L. Pushparaj , M. M. Shaijumon , A. Kumar , S. Murugesan , L. Ci , R. Vajtai , R. J. Linhardt , O. Nalamasu and P. M. Ajayan , *Proc. Natl. Acad. Sci. U. S. A.*, 2007, **104** , 13574 -13577 [CrossRef](#) [CAS](#) [PubMed](#)  .
23. F. Y. Su , C. H. You , Y. B. He , W. Lv , W. Cui , F. M. Jin , B. H. Li , Q. H. Yang and F. Y. Kang , *J. Mater. Chem.*, 2010, **20** , 9644 -9650 [RSC](#)  .
24. S. Flandrois and B. Simon , *Carbon*, 1999, **37** , 165 -180 [CrossRef](#) [CAS](#)  .
25. Y. P. Wu , E. Rahm and R. Holze , *J. Power S*